Atmos. Meas. Tech. Discuss., doi:10.5194/amt-2016-261, 2016
Manuscript under review for journal Atmos. Meas. Tech.
Published: 19 December 2016

Atmospheric Measurement Techniques Discussions

Characterisation of interferences to in-situ observations of $\delta^{13}CH_4$ and C_2H_6 when using a Cavity Ring Down Spectrometer at industrial sites.

Sabina Assan[1], Alexia Baudic[1], Ali Guemri[1], Philippe Ciais[1], Valerie Gros[1] and Felix R. Vogel[1]

[1]Laboratoire des Sciences du Climat et de l'Environnement, Chaire BridGES, UMR CNRS-CEA-UVSQ, Gif-sur-Yvette, Ile-de-France, 91191, France

Correspondence to: Sabina Assan (sabina.assan@lsce.ipsl.fr)

Abstract

The increase of atmospheric methane (CH_4) is the second largest contributor to the increased radiative forcing since the industrial revolution. Natural gas extraction and distribution is associated with CH_4 leaks of uncertain magnitude that has spurred interest for developing new methods to measure them. Using a CRDS instrument we evaluate two methane identification methods commonly used to better constrain emission estimates from natural gas leaks, namely stable isotope analysis and the ethane: methane ratio (C_2H_6:CH_4). Recently it has come to light that CRDS measurements of $\delta^{13}CH_4$ and C_2H_6 in the near infrared spectral domain are subject to cross sensitivities due to absorption from multiple gases. These sensitivities translate into biases in the retrieval of $\delta^{13}CH_4$ and C_2H_6 concentrations in air samples, and should thus be accounted for during data processing. Here we present extensive laboratory tests using two CRDS instruments to characterize their cross sensitivities and propose corrections to calculate unbiased $\delta^{13}CH_4$ and C_2H_6. Methane isotopic measurements were found to be subject to interference from elevated C_2H_6 concentrations (a secondary component in many natural gas types) resulting in heavier $\delta^{13}CH_4$ by +23.5‰ per ppm C_2H_6/ ppm CH_4. Measured C_2H_6 is subject to absorption interference from a number of other trace gases, the predominant being H_2O (with an average linear sensitivity of 0.9 ppm C_2H_6 per % H_2O in ambient conditions, meaning that the presence of H_2O causes the inference of too high C_2H_6 mixing ratios if no correction is applied). Yet, this sensitivity was found to be discontinuous with a strong hysteresis effect. Throughout the range of C_2H_6 concentrations measured in this study (0-5ppm C_2H_6), both CRDS instruments consistently measure concentrations double that reported by a GC, thus we have calculated a calibration factor of 0.5. To demonstrate the significance of the corrections we test the source identification methods on air measured at a natural gas compressor station. The presence of C_2H_6 in gas emissions at an average level of 0.3ppm was found to shift the isotopic signature by 2.5‰. We find that after correction and calibration the average C_2H_6:CH_4 ratio shifts by +0.06. These results indicate that when using such a CRDS instrument in conditions of elevated C_2H_6 for CH_4 source determination it is imperative to account for the biases discussed within this study.

Atmos. Meas. Tech. Discuss., doi:10.5194/amt-2016-261, 2016
Manuscript under review for journal Atmos. Meas. Tech.
Published: 19 December 2016

Atmospheric Measurement Techniques Discussions

1. Introduction

With increasing efforts to mitigate anthropogenic greenhouse gas emissions, opportunities to reduce leaks from fossil fuel derived methane ($ffCH_4$) is of particular importance as they currently account for approximately 30% of all anthropogenic methane emissions [Kirschke et al., 2013]. At present, technically feasible mitigation methods hold the potential to half future global anthropogenic CH_4 emissions by 2030. Of this mitigation potential more than 60% can be realised in the fossil fuel industry [Hoglund-Isaksson, 2012]. However for effective implementation, sources, locations and magnitudes of emissions must be well known.

The global increase in the production and utilisation of natural gas, of which methane is the primary component, has brought to light questions in regards to its associated fugitive emissions, i.e. leaks. Recent estimates of CH_4 leaks vary widely (1-10% of global production) [Allen et al., 2014] and US inventories of natural gas CH_4 emissions have uncertainties of up 30% [EPA, 2016]. To address this issue the ability to distinguish between biogenic and different anthropogenic sources is of vital importance. For this reason methane isotopes ($\delta^{13}CH_4$) are commonly used to better understand global and local emissions as demonstrated in a number of studies [Lamb et al., 1995, Lowry et al., 2001, Hiller et al., 2014]. The discrimination of sources with relatively close isotopic composition such as associated-oil gas and natural gas, whose isotopic signatures can be separated by only ~4 ‰ [Stevens et al., 1988], requires precise and reliable $\delta^{13}CH_4$ measurements.

Ethane (C_2H_6) is a secondary component in natural gas and can be used as a marker to distinguish between different CH_4 sources. Use of the C_2H_6:CH_4 ratio provides a robust identifier for the gas of interest. Recent findings in the US found coal bed C_2H_6:CH_4 ratios ranging between 0-0.045, while dry and wet gas sources displayed differing ratios of <0.06 and >0.06 respectively [Yacovitch et al., 2014, Roscioli et al., 2015].

Laser spectrometers, especially based on **C**avity **R**ing **D**own **S**pectroscopy (CRDS) are now a common deployment for site-scale CH_4 measurement campaigns [Yvon-Lewis et al., 2011, Phillips et al., 2013, Subramanian et al., 2015]. However, with the advent of such novel technologies, there lies the risk of unknown interference of laser absorption which can cause biases to measurements. Some examples of which are discussed in Rella et al., (2015) and many others [e.g. K.Malowany et al., 2015, Vogel et al., 2013, Nara et al., 2012]. Using a CRDS instrument we show that the presence of C_2H_6 is causing significant interference on the measured $^{13}CH_4$ spectral lines thus resulting in shifted reported $\delta^{13}CH_4$ values. We propose a method to correct these interferences, and test it on measurements of natural gas samples performed at an industrial natural gas site.

The CRDS instruments used throughout this study are Picarro G2201-i analysers (Picarro INC, Santa Clara, USA) whose measured gasses include CH_4, CO_2, H_2O, and, although not intended for use, C_2H_6. This model comprises two lasers, the first quantifies mole fractions of $^{12}CH_4$, $^{12}CO_2$ and $^{13}CO_2$, by measuring spectral lines roughly at 6057cm^{-1} whereas the second laser focuses on $^{13}CH_4$, H_2O and C_2H_6 mole fractions, measuring at approximately 6029cm^{-1}. The resulting spectrograms are fit with two non-linear models in order to determine concentrations; the primary fit is performed excluding the model function of C_2H_6 while the second includes this function thus adding

Atmos. Meas. Tech. Discuss., doi:10.5194/amt-2016-261, 2016
Manuscript under review for journal Atmos. Meas. Tech.
Published: 19 December 2016

Atmospheric Measurement Techniques Discussions

the ability to measure C_2H_6 [Rella et al., 2015]. Such a method for measuring C_2H_6 concentrations is crude, thus the uncalibrated C_2H_6 concentration data is stored in private archived files which until now have been used primarily for the detection of sample contamination. The measurements of $\delta^{13}CH_4$ and $\delta^{13}CO_2$ are calculated using the ratios of the concentrations of $^{12}CH_4$,$^{13}CH_4$, $^{12}CO_2$ and $^{13}CO_2$ respectively.

Presented here is an experimental procedure to correct the interference caused by C_2H_6 on the retrieval of $\delta^{13}CH_4$ using such a CRDS instrument for application to in-situ or continuous measurements of $\delta^{13}CH_4$ strongly contaminated by C_2H_6, i.e. in the vicinity of ffCH_4 sources. Literature suggests ethane mixing ratios ranging from 0.3 ppm to 3 ppm C_2H_6 for measurements taken within proximity of oil and gas leaks [e.g. Gilman et al., 2013, Jackson et al., 2014], while C_2H_6 in French and British background air stations is in the order of 1-2 ppb [Derwent et al., 2014, Waked et al., 2016]. Thus, our interference correction is designed for application to samples containing pure natural gas, or in the close proximity of leaks, i.e. suitable for emission factor and source apportionment studies. The step by step procedure of the experimental methods developed to quantify the cross sensitivities and the proposed calibration for $\delta^{13}CH_4$ and C_2H_6 are depicted in Fig. 1, and presented in detail in Sect. 2. Section 3 encompasses a discussion of the results, including analysis of the instrumental responses for two spectrometers with an evaluation of the stability and repeatability of the suggested corrections. Finally, field measurements were performed at a natural gas compressor station of which the aim was to identify emissions between two natural gas pipelines. In Sect. 5 the importance of the corrections for field measurements is demonstrated by applying our methods to data retrieved during this period while also revealing the instruments potential to measure C_2H_6.

2. Methods

Laboratory tests were conducted with the aim to characterize the instruments response to concentration changes in gasses found at fossil fuel sites (e.g. gas extraction or compressor stations). This includes the cross-sensitivities of CO_2, CH_4, and H_2O on C_2H_6 and the effect of concentration changes of C_2H_6 on $\delta^{13}CH_4$. It is likely for there to be additional gases with the potential for interference; in this study we focus on those which have been reported to have significant effect on C_2H_6 and $\delta^{13}CH_4$ measurements by Rella et al., (2015). We also define and describe a new procedure to calibrate both C_2H_6 and $\delta^{13}CH_4$.

In order to assess intra-instrument variability the majority of tests were undertaken with two instruments of the same model in parallel. To determine the stability over time, tests were repeated throughout the course of one year. In the following chapter the general setup used for the majority of experiments is described after which we enter a more detailed description of the processes involved in each step individually.

2.1 Experimental Setup:

2.1.1 Method:

Atmos. Meas. Tech. Discuss., doi:10.5194/amt-2016-261, 2016
Manuscript under review for journal Atmos. Meas. Tech.
Published: 19 December 2016

Atmospheric Measurement Techniques Discussions

Each cross sensitivity is measured by creating a gas dilution series designed to control the concentrations of the gas responsible for the interference in steps while keeping concentrations of the other gas components constant (in particular the component subject to interference). Thus, any shift in the measured concentrations of a (component) gas that has been kept constant allows us to characterise a bias due to a cross sensitivity which can be evaluated for a large range of concentrations. The experimental set-up used for such experiments includes two CRDS instruments (Picarro G2201-i) running in parallel in a laboratory at ambient conditions (25°C, 100m above sea level (a.s.l)). The instruments were used in iCO_2-iCH_4 auto switching mode, in which we consider only the 'high precision' mode of $\delta^{13}CH_4$ throughout the study. For the dilution series, a working gas is diluted in steps using a setup of two Mass Flow Controllers (MFC) (El-flow, Bronkhorst, Ruurlu, The Netherlands), as shown in Fig. 2. A T-junction splits the intended gas flow to both instruments; the total flow is greater than the flow drawn into the instruments, hence to maintain an inlet pressure close to ambient the setup includes an open split to vent additional gas. In order to assess variability and error, each experiment is repeated a minimum of 3 times consecutively. Each step within a dilution series is measured for an appropriate time to allow for stable measurement conditions (minimum 10 minutes) and optimal instrumental measurement uncertainties. During data processing initial data points are eliminated according to the observed settling time. To detect instrumental drift between experiments, a target gas is measured before commencing each dilution sequence. An overview of each cross interference targeted, with information on the gasses used and ranges spanned in laboratory tests can be found in Table 1.

2.1.2 Gases:

Throughout the experiments 4 categories of gas were used: a zero air gas with measured residual concentrations of <1ppm CO_2, <30ppb CH_4 , ≈170ppb CO, <1ppb C_2H_6 (Deuste-Steininger,Walldorf, Germany), working gases with variable concentrations of CO_2 and CH_4 in a natural air matrix (Deuste-Steininger,Walldorf, Germany), a C_2H_6 standard of 52 ppm in Nitrogen (National Physics Laboratory (NPL), Teddington, United Kingdom), and dried ambient air in 40L aluminium cylinders filled using an oil-free RIX compressor (RIX industries, Benicia, USA). Details of the gas mixture used in each dilution series depends on the response targeted within the experiment. Information can be found in Table 1 and are also discussed in further detail throughout this chapter.

2.2 Determination of C_2H_6 corrections from H_2O, CH_4 and CO_2 interference

The value of C_2H_6 based on the standard CRDS data processing package (hereafter, the raw value) is biased by cross-sensitivities with H_2O, CO_2 and CH_4 which must be identified and corrected before other corrections or calibrations can take place. For the three gasses targeted within this sub-section, C_2H_6 concentrations are consistently <1 ppb so that any shifts in the raw C_2H_6 is due to the cross sensitivity to other components in the measured samples. With the aim of altering the water vapour content of a sample, the experimental setup described in Fig. 2 was modified by incorporating a humidifier. The humidifier consists of a liquid flow controller (Liqui-flow, Bronkhorst, Ruurlu, The Netherlands) and a mass flow controller (El-flow, Bronkhorst, Ruurlu, The Netherlands) fed into a controlled evaporator mixer (CME) (Bronkhorst, Ruurlu, The Netherlands). The tube

Atmos. Meas. Tech. Discuss., doi:10.5194/amt-2016-261, 2016
Manuscript under review for journal Atmos. Meas. Tech.
Published: 19 December 2016

Atmospheric Measurement Techniques Discussions

departing the CME contains a gas flow of 2L/min and is heated to 40°C to prevent any condensation. A short description and diagram of the humidifying bench can found in Laurent et al., (2015).

The H_2O interference on C_2H_6 was measured by using the humidifier to vary the H_2O content of zero air gas in the range of 0.25%- 2.5% H_2O, representing the range of real world conditions. The humidifier set up cannot reliably reach humidity's below 0.2% H_2O, a range frequently reached when measuring cylinders or dried air. Therefore to focus on H_2O content within this low range, a second experiment was conducted in which a H_2O scrubber (Magnesium Perchlorate, Fisher Scientific, Loughborough, UK) was connected to the CRDS instrument inlet while measuring ambient air. As the efficiency of the scrubber decreases over time, a slow increase of H_2O spanning low concentrations in the range of 0%-0.5% can be observed.

The CH_4 interference on C_2H_6 was measured by creating a dilution series of variable CH_4 content using zero air and a working gas of 6ppm CH_4, 360ppm CO_2, 310ppb N_2O and 50ppb CO in natural air. Methane concentrations ranged from 0 – 6ppm. To keep other causes of interference at a minimum the gas mixture passed through two scrubbers; the first a CO_2 scrubber (Ascarite(ii), Acros Organics, USA), and the second a H_2O scrubber (Magnesium Perchlorate, Fisher Scientific, Loughborough, UK). As an independent check on the linearity of the response functions each dilution sequence was repeated at two different humidities, 0% H_2O and 1% H_2O respectively.

The CO_2 interference on C_2H_6 was measured with a dilution series ranging 0-1500ppm CO_2 created by mixing zero air and a working gas of 2000ppm CO_2, 1.7ppm CH_4 and 50ppb CO in natural air. Any interference due to CH_4 was accounted for during data processing. This test was repeated at 5 different humidities ranging between 0-1.5% H_2O.

2.3 C_2H_6 calibration setup

In order to correctly use the C_2H_6 data from CRDS instruments, the data must be calibrated to an internationally recognised scale. To achieve this, the set up described in Sect. 2.1 was modified to include the ability to fill removable samples whose concentrations could be independently verified. Hence 1L glass flasks were incorporated into the setup, as shown in Fig. 2. A gas mixture using the C_2H_6 standard and an ambient air cylinder was created via two MFCs before passing through the flask on its way to the instruments inlets. Each step in the dilution series requires an individual flask, which was flushed for 20 minutes and then analysed for 10 minutes with an average precision of 0.02ppm C_2H_6 on the CRDS instrument. The flask is subsequently sealed and removed for analysis on a Gas Chromatograph (GC) [Chrompack Varian 3400, Varian Inc, USA] which uses National Physics Laboratory (NPL) standards, and has an uncertainty better than 5%. The system is described in more detail in Bonsang and Kanakidou (2001).

In total 17 flasks were filled with gas mixtures spanning from 0ppm to 5ppm C_2H_6, covering the range expected near a leak of ffCH_4. In order to calibrate the linearity of the response at very high concentrations which may be expected from pure natural gas samples we conducted a measurement at 100% of the C_2H_6 standard (52 ppm ± 1 ppm).

Atmos. Meas. Tech. Discuss., doi:10.5194/amt-2016-261, 2016
Manuscript under review for journal Atmos. Meas. Tech.
Published: 19 December 2016

Atmospheric Measurement Techniques Discussions

2.4 Determining the correction for $\delta^{13}CH_4$

Measured $\delta^{13}CH_4$ is altered in the presence of C_2H_6. To understand the magnitude of this effect, experiments were conducted using the method described in Sect. 2.1. The dilution series uses the C_2H_6 standard and a cylinder filled with ambient air, i.e. with a negligible C_2H_6 mixing ratio (<1 ppb) to create concentration values spanning from 0-4 ppm C_2H_6. As there is only one source of CH_4 in the experiment, the addition of C_2H_6 should not affect the value of $\delta^{13}CH_4$, hence any change seen is an apparent shift of $\delta^{13}CH_4$ due to C_2H_6 interference. This concentration range was chosen as it encompasses a C_2H_6:CH_4 ratio of 0 to 1, well within the likely range to be measured from fossil fuel sources [Yacovitch et al., 2014].

2.5 Calibration of $\delta^{13}CH_4$

The reported $\delta^{13}CH_4$ was calibrated to Royal Holloway University of London (RHUL) scale using 4 calibration gases spanning -25‰ to -65‰ that were created by different dilutions of pure CH_4 and CO_2 with ambient air of which aliquots were measured multiple times by Isotope Ratio Mass Spectrometry (IRMS) at RHUL. The precision for $\delta^{13}CH_4$ obtainable with this IRMS is reported as 0.05‰, detailed information on the measurement system can be found in Fisher et al. (2006). The calibration factor is determined from a linear regression and calibrations were performed before and after the laboratory experiments. To ensure the calibration is reliable, it is repeated 3 times over a period of 3 days. The mean isotopic values of each repetition are all included within one linear regression under the assumption that the system does not vary significantly over this period. A target gas was measured regularly to track any drift in $\delta^{13}CH_4$ and to act as an independent check on the quality of the calibration.

3. Results and Discussion:

This study focuses on determining a reliable correction and calibration scheme for a Picarro G2201-i when measuring methane sources with C_2H_6 interference. Findings from the experiments described in Sect. 2 are discussed in detail here.

In order to calibrate $\delta^{13}CH_4$ and C_2H_6 values, there are a series of corrections that must take place (see Fig. 1). The initial correction to be applied is on C_2H_6 due to interference from CH_4, CO_2 and H_2O. Particular emphasis is placed on this correction due to the discovery of significant non-linear behaviour in the presence of H_2O, CH_4 and CO_2 in the sample gas. Once the C_2H_6 has been corrected, the calibration of C_2H_6 using independent GC measurements, the C_2H_6 interference correction on $\delta^{13}CH_4$ and finally the calibration of $\delta^{13}CH_4$ can be effected.

For our results to be applicable to future studies we examine the inter-instrument variability, stability over time, compare our results to current literature and discuss the uncertainties attributed to our results. Throughout this study we refer to raw, uncorrected C_2H_6 and $\delta^{13}CH_4$ concentrations as "reported" to highlight that they may be influenced by interferences and have not yet undergone correction treatment. Within this section often negative C_2H_6

Atmos. Meas. Tech. Discuss., doi:10.5194/amt-2016-261, 2016
Manuscript under review for journal Atmos. Meas. Tech.
Published: 19 December 2016

198 concentrations are mentioned, we note that this is the "reported" C_2H_6 concentration by the instrument. Unless
199 otherwise stated, the standard deviation reported is calculated from one minute averages and depicted as error bars
200 within figures.

201 **3.1. Correcting reported C_2H_6**

202 **3.1.1 H_2O interference on C_2H_6**

203 The effect of water vapour on reported C_2H_6 was determined by performing experiments in which the humidity of
204 zero air was varied between 0-2.5% (as described in Sect. 2.2). H_2O content was found to be the dominating source
205 of interference to reported C_2H_6; its presence decreases the reported concentration of C_2H_6 with increasing H_2O
206 concentration. Furthermore we have found that the response function exhibits a hysteresis effect, which, although
207 small, can be considerable when changing from dry to undried air samples (between dry calibration gas and undried
208 ambient air). Figure 3 shows the differing response functions obtained when measuring dried (dark blue markers)
209 or undried (light blue markers) ambient air during the night preceding the experiment. When the CRDS instrument
210 measures dry air prior to the experiment, a discontinuity is observed at 0.16% H_2O. Figure 4a shows this effect in
211 more detail; prior to 0.16% H_2O the response function exhibits a stable linear response. The correction within this
212 low range was found to be the same for both instruments, 0.44 ± 0.03 ppm C_2H_6/ % H_2O. After passing the 0.16%
213 H_2O threshold the response exhibits a discontinuity whose magnitude and subsequent slope are also dependent on
214 the air moisture beforehand. This can also be seen in Fig. 4a whereby two repetitions (A and B depicted by dark and
215 light blue points respectively) experience a difference in the magnitude of the discontinuity of 0.1ppm in reported
216 C_2H_6. The discontinuity is seen to occur when the instrument passes the 0.16% H_2O threshold, whether this be when
217 moving from dry to wet air, or vice versa (see Fig. 4b). If measuring undried air before the experiment, the
218 interference due to H_2O can be described well by a linear response (blue markers in Fig. 3), and potentially causes
219 large biases from the true C_2H_6. For example if measuring at 1% H_2O both instruments display a change in reported
220 C_2H_6 of approximately -0.9ppm. Individually the response function calculated for instruments *CFIDS 2072* and
221 *2067* differed slightly showing -0.72 ± 0.03 ppm C_2H_6/%H_2O and -1.00 ± 0.01 ppm C_2H_6/%H_2O with R^2 values of
222 0.98 and 0.99 respectively. The hysteresis effect is not as evident within this range, however a shift in the slope of
223 0.1 ppm C_2H_6/%H_2O has been measured between the first and third repetition of the experiment.

224 **3.1.2 CO_2 interference on C_2H_6**

225 First tests revealed that the CO_2 interference on C_2H_6 is not fully independent of the H_2O levels of the sample.
226 Therefore, the correction of the CO_2 interference on C_2H_6 was examined extensively at varying H_2O water vapour
227 levels. The set-up of these experiments has been discussed within the Sect. 2, for which an example of the time
228 series can be seen in Fig. 5. The H_2O content was set at four different water vapour levels (0%, 0.5%, 1% and 1.5%)
229 and dried air was measured between each level to minimise the hysteresis effect observed within the H_2O correction
230 tests. For each H_2O level, a CO_2 dilution series (of minimum 3 concentrations) was created in order to detect any
231 covariance on the CO_2 interference arising due to water vapour content. For both instruments an increase in the CO_2

Atmos. Meas. Tech. Discuss., doi:10.5194/amt-2016-261, 2016
Manuscript under review for journal Atmos. Meas. Tech.
Published: 19 December 2016

Atmospheric Measurement Techniques Discussions

concentration results in lower reported values of C_2H_6 and it is furthermore apparent, that the magnitude of this interference is dependent on air humidity. For a dry sample gas (H_2O <0.16% - demonstrated in the left hand column of Fig. 6), the interference for both instruments is found to be highly stable and well characterised by a linear slope of $1x10^{-4} \pm 1x10^{-5}$ $ppmC_2H_6/ppmCO_2$ with a R^2 value of 0.9. In contrast, for water vapour levels ≥ 0.5% H_2O (see right hand column of Fig. 6) measurements exhibit a higher scatter between repetitions. This is mainly attributed to a drifting intercept however the experiments also show a smaller R^2 of 0.8. The slope obtained for each repetition is largely within observed uncertainties, thus we combined the results to obtain a characteristic linear slope of $3.8x10^{-4} \pm 1x10^{-5}$ $ppmC_2H_6/ppmCO_2$ and $3.9x10^{-4} \pm 1x10^{-5}$ for ≥0.5% water vapour for instruments *CFIDS 2072* and *2069* respectively. Therefore, measuring undried ambient air the presence of CO_2 at a level in the range of 400 ppm will typically induce a shift in the reported C_2H_6 of approximately -0.15 ppm C_2H_6, whereas if the air is dried the reported shift is much smaller, being approximately of -0.04ppm C_2H_6.

3.1.3 CH_4 interference on C_2H_6:

The CH_4 effect on C_2H_6, as shown in Fig. 7, is less prominent by at least an order of magnitude than both the H_2O and CO_2 interferences. At dried ambient CH_4 concentrations a typical change in reported C_2H_6 of approximately -0.008ppm is observed within both instruments. Dried air experiments show a high scatter of points between repetitions, when combining all data points an R^2 value of 0.4 and 0.6 for instruments *CFIDS 2072* and *2067* respectively is calculated. Despite its large uncertainty the data suggests both instruments display a similar response with a statistically significant slope. In light of this we use a weighted mean to calculate a linear response of $5x10^{-3} \pm 4x10^{-3}$ $ppmC_2H_6/ppmCH_4$ for dry air measurements for *CFIDS 2067*, and $7x10^{-3} \pm 5x10^{-3}$ $ppmC_2H_6/ppmCH_4$ for *CFIDS 2072*. The results obtained at 1% H_2O show little correlation (as shown in the right hand column of Fig. 7), with both instruments displaying a R^2 value of 0.2. An ANOVA test suggests the slopes are not significantly different from zero, thus we omit a CH_4 correction for this case.

3.1.4 Combining the CO_2, CH_4 and H_2O correction on C_2H_6

To fully take into account all (known) C_2H_6 cross-sensitivities the corrections to reported C_2H_6 need to be combined. As we have found the instrument behaviour to be not strictly linear (independent) for different component concentrations and as the discontinuity in reported C_2H_6 for 0.16% H_2O and its subsequent slope is hard to predict, we do not calculate a correction for the effect. We rather choose to report correction coefficients for the two found linear regimes, i.e. for continuous measurements with sample humidities below 0.16% and sample humidities above 0.16%. Within each range the proposed correction formula is given as:

$$[C_2H_6]_{CORRECTED} = [C_2H_6]_{RAW} + A^*[H_2O] + B^*[CH_4] + C^*[CO_2] \quad \text{Eq. (1)}$$

If the humidity is limited to **less than** 0.16% before and during measurements, $A=0.44 \pm 0.03$ $ppmC_2H_6/\%H_2O$, $B=5x10^{-3} \pm 4x10^{-3}$ $ppmC_2H_6/ppmCH_4$, $C=1x10^{-4} \pm 1x10^{-5}$ $ppmC_2H_6/ppmCO_2$. Both instruments demonstrated good agreement for all the correction factors calculated at <0.16% H_2O.

Atmos. Meas. Tech. Discuss., doi:10.5194/amt-2016-261, 2016
Manuscript under review for journal Atmos. Meas. Tech.
Published: 19 December 2016

Atmospheric Measurement Techniques Discussions

Corrections for measurements undertaken at concentrations **higher than or equal to** 0.16% H_2O are: A=0.7 ± 0.03 ppmC_2H_6/%H_2O, B=0 ppmC_2H_6/ppmCH_4, C=3.8x10^{-4} ± 2x10^{-5} ppmC_2H_6/ppmCO_2 for *CFIDS 2072* and A=1 ± 0.01 ppmC_2H_6/%H_2O, B=0 ppmC_2H_6/ppmCH_4, C=3.9x10^{-4} ± 2x10^{-5} ppmC_2H_6/ppmCO_2 for *CFIDS 2067*.

3.2 C_2H_6 calibration

To make use of the corrected CRDS based C_2H_6 it should be calibrated to match an internationally recognised scale. To calibrate the C_2H_6 to such a scale, whole-air samples were measured by CRDS and independently on a calibrated Gas Chromatograph, as discussed within Sect. 2. The calibration factor is determined by comparing the corrected C_2H_6 resulting from CRDS and C_2H_6 as confirmed by the GC, plotted in Fig. 8a. The relationship was found to be linear throughout the range of 0-5ppm C_2H_6 with a slope of 0.505±0.007 and 0.52 ± 0.01 for instruments *CFIDS 2072* and *2067* respectively. The results are reported in Table 2 from which we can see the intercept of the calibration for instrument *CFIDS 2072* shifts between the experiment in February and that in October, while the slope remains constant over long periods of time. The change in the intercept is attributed to a C_2H_6 baseline drift which we have monitored over time using regular target gas measurements, example given in Fig. 8b. To account for this drift, and any elevated baselines (such as that of CFIDS 2067 – see Table 2) a regular measurement of a working gas is necessary. By tracking the baseline drifts using this working gas (which can also serve as a target gas for other gases) we can calculate the instrument offset. For the full calibration we thus suggest using Eq. (2), where D is the calibration factor (slope) for the instrument, i.e. for *CFIDS 2072* D= 0.505±0.007 and Δ [WGS] the baseline drift determined using the working gas.

$$[C_2H_6]_{calibrated}=D*([C_2H_6]_{corrected}-\Delta[WGS]) \quad \text{Eq. (2)}$$

3.3 $\delta^{13}CH_4$ correction

By measuring the shift of the reported $\delta^{13}CH_4$ in C_2H_6-contaminated samples, we have observed that the instrument reports heavier values of $\delta^{13}CH_4$ in the presence of C_2H_6. The shift is a result of increased reported $^{13}CH_4$ in samples containing C_2H_6 (see Fig. 9). This is most likely caused by the overlapping of spectral lines within the 6029 wavenumber region [Rella et al., 2015]. We calculate the $\delta^{13}CH_4$ correction by taking the slope of $\Delta\delta^{13}CH_4$ (the difference between the reported $\delta^{13}CH_4$ and the initially reported one of the C_2H_6-free gas) and the corrected C_2H_6 to CH_4 ratio. The ratio is used to permit the calculation of the $\delta^{13}CH_4$ response function per ppm CH_4 as the magnitude of interference is dependent on CH_4 concentration [Rella et al., 2015]. The significance of the interference on $\delta^{13}CH_4$ concentrations is illustrated in Fig. 10; as the C_2H_6:CH_4 ratio increases, the change in the reported $\delta^{13}CH_4$ increases linearly. Results obtained from tests carried out throughout the year, for both instruments are noted in Table 3, and plotted in Fig. 10. The correction equation can be expressed as:

$$[\delta^{13}CH_4]_{CORRECTED}= [\delta^{13}CH_4]_{RAW} - E * C_2H_{6\,CORRECTED}/ CH_4 + F \quad \text{Eq. (3)}$$

where E is the slope of the response function and F is the intercept. E and F are +23.6 ± 0.4 ‰ ppm CH_4 /ppm C_2H_{64} and approximately +0.4±0.2‰ for instrument *CFIDS* 2072 and +23.3 ± 0.7‰ ppm CH_4 /ppm C_2H_6 and

Atmos. Meas. Tech. Discuss., doi:10.5194/amt-2016-261, 2016
Manuscript under review for journal Atmos. Meas. Tech.
Published: 19 December 2016

Atmospheric Measurement Techniques Discussions

approximately -2.4 ±0.4‰ for instrument *CFIDS 2067* respectively. These corrections contain the inherent $\delta^{13}CH_4$ offset of the instrument. When calibrating the $\delta^{13}CH_4$ to a known scale (as described in Sect. 2.5) any instrumental offset will be incorporated within the calibration, therefore the correction equations can be simplified to:

$$[\delta^{13}CH_4]_{CORRECTED} = [\delta^{13}CH_4]_{RAW} - E * C_2H_{6\,CORRECTED} / CH_4. \quad \text{Eq. (4)}$$

Also highlighted in Fig. 10 is the typical measurement range for the majority of $ffCH_4$ sources related to *dry and wet* natural gas relative to calibrated C_2H_6/CH_4 ratios given on the upper abscissa; whereby *dry* gas refers to natural gas that occurs in the absence of condensate/liquid hydrocarbons (C_2H_6:CH_4 = 1-6%) while *wet* gas typically contains higher concentrations of complex hydrocarbons (C_2H_6:CH_4 >6%) [Yacovitch et al., 2014]. It is clear that within this range the bias on methane isotopic signatures is significant; dry gas will alter the reported $\delta^{13}CH_4$ by 0.8-4‰, while wet gas can cause a shift of up to 13‰ depending on its C_2H_6:CH_4 ratio.

3.4 $\delta^{13}CH_4$ calibration

Full instrument calibrations as described in Sect. 2.4 were performed once in 2014 and 2015. The $\delta^{13}CH_4$ values obtained for the calibration gases by RHUL are measured by IRMS and are therefore not subject to interferences. The calibration gas aliquots were measured with an average standard deviation of 0.03‰. To calibrate $\delta^{13}CH_{4\,CORRECTED}$, the $\delta^{13}CH_{4\,CORRECTED}$ was calculated for each calibration gas and used within the linear regression. The calibrations were linear with R^2>0.99 on both occasions and no change (within our uncertainties) was observed between the two tests. By measuring an ambient air target regularly we later detected a shift in the $\delta^{13}CH_4$ baseline. Two further calibrations were performed in 2016 to assess this incident which confirmed that the offsets of the linear regressions were significantly shifted, while the slopes agreed well with previous calibrations. Therefore to account for a baseline drift it is important to measure a target gas regularly and amend the offset of the calibration equation accordingly.

3.5 Typical instrumental performance and uncertainties

Our CRDS is frequently used for different field deployments and in order to assess the potential benefit of co-located $\delta^{13}CH_4$ and C_2H_6 observations we need to evaluate the typical performance here. In order to characterize the repeatability of the C_2H_6 measured by the CRDS instrument we have measured several targets and monitored the changes of the reported C_2H_6 signal over time. The raw signal is a measurement every 3 seconds, which displays on average a standard deviation of 90 ppb. By aggregating the data to 1 minute intervals the precision can be improved and a standard deviation of 20 ppb is reached, while 30 minute aggregation reduces this further to 8 ppb. Furthermore, when measuring the 52 ppm C_2H_6 standard, the 1 minute standard deviation is 180 ppb. Therefore, by assuming a linear relationship, we have calculated a typical performance for 1 minute averages of 20 ppb +/- 0.3% of reading.

Of course, there are some substantial uncertainties attributed with the C_2H_6 correction and calibration which need to be accounted for when discussing the uncertainty of the calibrated C_2H_6 concentrations. With regards to the C_2H_6

Atmos. Meas. Tech. Discuss., doi:10.5194/amt-2016-261, 2016
Manuscript under review for journal Atmos. Meas. Tech.
Published: 19 December 2016

Atmospheric Measurement Techniques Discussions

correction for 1 minute averages, if measuring dried ambient air the propagation of uncertainties are negligible with respect to the raw instrumental precision (20ppb). However if using 30 minute averages the uncertainty augments from 8ppb to 10ppb due to the propagation of uncertainties associated with the correction coefficients. Elevated CH_4, CO_2 and H_2O signals (>5ppm, >1000ppm,> 0.2% respectively) will induce increased C_2H_6 uncertainty regardless of aggregation time. After calibration we have found that the uncertainty increases to $2^{1/2}$ times that of the corrected C_2H_6, so at ambient air concentrations calibrated C_2H_6 has an uncertainty of 30ppb.

The repeatability of $\delta^{13}CH_4$ for 1 minute averages on our instrument is a standard deviation of 0.66‰. Again the standard deviation is reduced to 0.29‰ and 0.09‰ by aggregating the raw data for 5 minutes and 30 minutes, respectively. For the correction of $\delta^{13}CH_4$ due to C_2H_6, error propagation of the factors applied in Eq. (4) must be taken into account. Therefore, at ambient concentrations, the uncertainty of a 1min average will increase to 0.9‰.

3.6 Generalisability of corrections and calibrations

The experiments in this study were repeated multiple times and performed on different instruments to better understand how the instrument responses change over time and how they vary between instruments.

The C_2H_6 correction and calibration, and $\delta^{13}CH_4$ correction experiments were repeated on *CFIDS 2072* over the course of a year to determine any temporal drifts.

The coefficients of the C_2H_6 correction were examined over a 4 month period. Methane, Carbon dioxide and water vapour coefficients for dried gas displayed no noticeable variation over this time frame. Both CH_4 and CO_2 coefficients for undried gas also showed good stability throughout this period, however the undried H_2O coefficient is seen to vary significantly (±0.1 ppmC_2H_6/%H_2O). As discussed previously, the H_2O correction is subject to a hysteresis effect, which makes analysis of its long term variation difficult. As we did not find a clear temporal pattern of the variations we therefore suggest that this coefficient is not likely to be time dependant.

The calibration of C_2H_6 was calculated twice within a 9 month period (see Table 2). No variation of the slope of the response function is observed within this time frame. The intercept is prone to drift in time as discussed previously.

The $\delta^{13}CH_4$ correction has been examined three times throughout a 6 month period (see Table 3), during which time the analyser had been switched off and relocated on several occasions. The variability of the slope observed over 6 months is 1‰ ppmC_2H_6/ppmCH_4. Given that the error attribution of each experiment is approximately ± 1‰ ppmC_2H_6/ ppmCH_4, this variability is not statistically significant. The intercepts show good agreement with no variation outside the expected uncertainties.

All experiments were applied to two instruments of the same model in order to infer the variability of the aforementioned correction and calibration factors between them. Both CRDS instruments showed good agreement for all calculated C_2H_6 correction coefficients with the exception of the undried H_2O coefficient at >0.16% H_2O. For

Atmos. Meas. Tech. Discuss., doi:10.5194/amt-2016-261, 2016
Manuscript under review for journal Atmos. Meas. Tech.
Published: 19 December 2016

Atmospheric Measurement Techniques Discussions

this coefficient we calculate a difference of 0.3 ppmC_2H_6/%H_2O between that of *CFIDS* 2072 and *CFIDS 2067*. The variance may be the consequence of spectrometer differences, a long-term hysteresis effect or due to differences in their past use up to our tests (mostly dried samples on CFIDS 2072 and mostly undried samples for CFIDS 2067).

The slopes derived for the C_2H_6 calibration of both instruments correspond well, with no significant difference seen between the two. The intercepts differ by approximately 0.6 ppm, thus suggesting distinct difference between intra-instrumental C_2H_6 baselines.

The slopes of the $\delta^{13}CH_4$ correction were found to be in good agreement between the two instruments. Where the instruments differ is with regards to their $\delta^{13}CH_4$ baseline, thus causing the observed disparity in intercept (seen in Table 3) of approximately 3‰.

To the best of our knowledge, at this time there is only one published study reporting on a correction due to C_2H_6 interference on an isotopic Picarro analyser. Rella et al., (2015) have studied the interference using a Picarro G2132-i, a high precision CH_4 Isotope-only CRDS analyser which uses similar analysis algorithms and spectral regions as that of the Picarro G2201-i. Rella et al., (2015) obtained C_2H_6 correction parameters of A=0.658 ppm C_2H_6/ ppm H_2O, B=5.5 ± 0.1 x 10^{-3} ppm C_2H_6/ ppm CH_4, C=1.44 ± 0.02 x 10^{-4} ppm C_2H_6/ ppm CO_2 in 2015. Factors B and C for CH_4 and CO_2 respectively agree well with the dried air coefficients attained within this study, however the values are not specified to be dry or wet factors. The H_2O coefficient, as suggested by Rella et al., (2015) differs to both that of *CFIDS* 2072 and *CFIDS 2067* but confirms the variability of this factor between instruments when measuring undried air samples. The discontinuity observed within the H_2O response for dried air samples was not discussed in Rella et al., (2015). Lastly, Rella et al., (2015) report a correction factor for $\delta^{13}CH_4$ of 35‰ ppm CH_4 /ppm C_2H_6. Although comparable, this differs to that calculated in our study by approximately 10‰ ppm CH_4 /ppm C_2H_6. The reason for this disparity is not clear, we suggest that because the G2132-i analyser used by Rella et al., (2015) is devoted to CH_4 Isotope-only measurements it may be affected by C_2H_6 to a different extent.

4. Source Identification at a Natural Gas Compressor Station

In order to quantify the effect of C_2H_6 contamination in a real world situation, we have applied the corrections and calibrations discussed in this paper to measurements taken at a natural gas site, with the aim of distinguishing emissions between two natural gas pipelines. In the following section we demonstrate the effect of C_2H_6 interference correction on $\delta^{13}CH_4$ at a fossil fuel site, as well as discuss the alternative approach of using calibrated C_2H_6:CH_4 ratios to distinguish source signatures, a method which has not been previously tested on a Picarro G2201-i.

4.1. Description of field campaign

4.1.1. Site description

Atmos. Meas. Tech. Discuss., doi:10.5194/amt-2016-261, 2016
Manuscript under review for journal Atmos. Meas. Tech.
Published: 19 December 2016

Located in an industrial park in northern Europe, the campaign took place at a natural gas compressor station in summer 2014. Such stations serve the distribution of natural gas; its key purpose is to keep an ideal pressure throughout the transmission pipelines to allow continuous transport from the production and processing of natural gas to its use. The compressor site visited comprises two major pipelines with their corresponding compressors. The two pipelines carry gas of different origins to the site, where after pressurisation, they are combined for further transmission. The site topography is flat and open with the surrounding area as predominantly farm land and close proximity to a major road. FFCH_4 emissions were expected to emanate from various sources on site such as the compressors, methane slip from turbines, and fugitive emissions due to the high pressure of gas [Roscioli et al., 2015]. Other possible methane sources in the nearby region were identified as traffic and agriculture.

4.1.2 Continuous measurements of CH_4, $\delta^{13}CH_4$ & C_2H_6

Two instruments were utilised for continuous measurements throughout the two week field campaign: a CRDS instrument (*CFIDS 2072*, characterised in detail in previous sections) and an automatic Gas Chromatograph with a Flame Ionization Detector (GC-FID) (Chromatotec, Saint-Antoine, France) measuring VOCs (light fraction C_2-C_6 hydrocarbons), described in detail in Gros et al., (2011). Both were located at a distance of approximately 200m-400m from both the pipelines and compressors. A synchronised time series of both instruments was achieved by locating the two inlets beside one another and time stamped measurements.

The air measured by the CRDS instrument was dried consistently to <0.16 % H_2O using a Nafion (Perma Pure LLC, Lakewood, USA). The $\delta^{13}CH_4$ was calibrated using the method described previously in Sect. 2. 20 minute measurements of two calibration gases were made every two days to calibrate the CH_4 and CO_2 data and to track any drift in the isotopes. A C_2H_6 free working gas was measured every 12 hours and used simultaneously as a target gas for the calibration of CH_4 and CO_2, and to track any drift in the C_2H_6 baseline for the calibration of C_2H_6.

The GC-FID was calibrated at the beginning and end of the campaign using a certified standard gas mixture (NPL, National Physics Laboratory, Teddington, UK). The sampling time is a 10 minute average every half an hour; 10 minutes of ambient air is measured after which the following 20 minutes are used to analyse the input.

4.1.3 Grab sample measurements of CH_4, $\delta^{13}CH_4$ & C_2H_6 in pure natural gas samples

Grab samples of pure natural gas were taken of both pipelines, with the aim of characterizing the two differing gas supplies. The 0.8L stainless steel flasks were evacuated prior to sampling to a pressure of the order of 10^{-6} mbar, after which they were filled to ambient pressure when sampling. The flasks were measured independently in the laboratory with a manual GC (described in Sect. 2.4) and, after dilution with zero air by the CRDS instrument.

4.2 Impact of C_2H_6 on $\delta^{13}CH_4$ observations at the field site

To quantify the effect of C_2H_6 interference on $\delta^{13}CH_4$ a total of 16 events were selected from the two week field campaign, whose criteria was defined as a peak exhibiting both increasing CH_4 concentrations and a change in

Atmos. Meas. Tech. Discuss., doi:10.5194/amt-2016-261, 2016
Manuscript under review for journal Atmos. Meas. Tech.
Published: 19 December 2016

428 $\delta^{13}CH_4$ signature for a minimum of 1 hour. Two such events are plotted in Fig. 11. Event 1 represents the majority
429 of events measured during the field campaign, in which CH_4 and C_2H_6 are well correlated. This particular event has
430 a maximum concentration of 11ppm CH_4 and 0.6ppm C_2H_6. On average the selected events have peak concentrations
431 of 5ppm CH_4 and 0.3ppm C_2H_6. The methane isotopic signature was characterized using the Miller-Tans method
432 [Miller & Tans, 2003], in which $\delta^{13}CH_4$* CH_4 values are plotted against CH_4 to calculate the isotopic signature of
433 the methane source in situations where the background is not constant. In order to avoid bias stemming from using
434 Ordinary Least Squared (OLS) regression, the York least squares fitting method was implemented thus taking into
435 account both the X and Y error [York, D. 1968]. All events excluding one were found to have $\delta^{13}CH_4$ signatures
436 characteristic of natural gas, corresponding on average to -40‰. A singular event (Event 2 plotted in Fig. 11) was
437 detected with a $\delta^{13}CH_4$ signature of -59‰ ± 1.5‰. Such a signature suggests a biogenic source and, when examining
438 this event further with wind data, the source is likely to be cattle emissions.

439 If the data is left uncorrected, sources containing C_2H_6 substantially bias the calculated isotopic signature of CH_4
440 events. This is demonstrated in Fig. 11 where, for Event 1, the slope of points after C_2H_6 correction (in blue) is
441 shifted in comparison to the slope derived from points left uncorrected (in red); signifying a modification of the
442 $\delta^{13}CH_4$ signature. Corrected $\delta^{13}CH_4$ suggests a signature of -40.0‰ ± 0.1‰, while uncorrected values imply -37.8‰
443 ± 0.08 ‰. When no C_2H_6 is present, i.e. Event 2, there is no disparity between the raw and corrected $\delta^{13}CH_4$ slope,
444 resulting in a $\delta^{13}CH_4$ signature of -59‰ ± 1‰ for both methods. For the 15 natural gas related events, the average
445 shift induced due to uncorrected data is 2‰. Consequently the bias in isotopic signatures due to C_2H_6 means that
446 uncorrected data will always overestimate the source, when a simple two end-member mixing model between is
447 applied.

448 **4.3 Continuous field measurements of ethane**

449 As we have established the routine to correct and calibrate the reported C_2H_6 of our CRDS we can now use it for
450 continuous observations, which adds to our ability to interpret the source of a given CH_4 enhancement. As an
451 independent verification of the CRDS performance we compared two time series of C_2H_6 which were measured
452 simultaneously by the CRDS and GC-FID during the natural gas field campaign by using a co-located air inlet. The
453 CRDS data was averaged to identical time stamps as the GC-FID, i.e. a 10 minute average every 30 minutes. From
454 which we calculated a Root Mean Squared Error (RMSE) of 13 ppb. Given the precision of C_2H_6 measured by the
455 CRDS instrument is 10 ppb for 10 minute averages, and the uncertainty on the GC-FID is 15%, we conclude that
456 this is extremely good agreement.

457 Furthermore, the flask samples, taken on the 4th of July 2014, were measured by the CRDS to have a C_2H_6: CH_4
458 ratio of 0.074 ± 0.001 ppm C_2H_6 /ppm CH_4 and 0.046 ± 0.003 ppm C_2H_6 /ppm CH_4 for the gas within Pipeline 1 and
459 Pipeline 2 respectively. That same day gas quality data from the onsite GC recorded a C_2H_6: CH_4 ratio of 0.075 ppm
460 C_2H_6 /ppm CH_4 and 0.048 ppm C_2H_6 /ppm CH_4 respectively. Although the error associated with the later figures is
461 unknown, the strong agreement between the two verifies our correction and calibration strategy of C_2H_6.

Atmos. Meas. Tech. Discuss., doi:10.5194/amt-2016-261, 2016
Manuscript under review for journal Atmos. Meas. Tech.
Published: 19 December 2016

Atmospheric Measurement Techniques Discussions

4.4 Use of continuous observations of C_2H_6: CH_4 by CRDS

The instruments capability to now measure interference corrected and calibrated C_2H_6 opens the door for using another proxy for source apportionment, namely the C_2H_6:CH_4 ratio [Yacovitch et al., 2014, Roscioli et al., 2015, Smith et al., 2015]. Using this ratio to distinguish between ffCH_4 sources is a method of growing interest, partly due to the distinct difference in C_2H_6:CH_4 ratio between facilities and sources thus permitting easy source identification. The C_2H_6:CH_4 ratio that characterises each source is determined by the slope of the C_2H_6 to CH_4 relationship. This method was applied to the 16 events identified within the natural gas field campaign, again using the York linear regression method taking into account both X and Y error. Two examples of this method are displayed in the bottom panel of Fig. 11. Event 1, representing a natural gas emission has a measured C_2H_6: CH_4 ratio of 0.068 ± 0.002 ppm C_2H_6 /ppm CH_4 suggesting a wet gas source. Biogenic events, such as Event 2 are absent of C_2H_6 (within our detection limit) thus resulting in a C_2H_6: CH_4 ratio of 0 ± 0.2 ppm C_2H_6 /ppm CH_4. Excluding the biogenic event, on average the 15 natural gas emissions detected have a weighted mean C_2H_6: CH_4 ratio of 0.069 ppm C_2H_6 /ppm CH_4 with an average uncertainty on each event of 0.006 ppm C_2H_6 /ppm CH_4. This figure agrees well with the median value for conventional gas ratios measured by Roscioli et al., (2015).

If the C_2H_6 data is left uncorrected and un-calibrated the C_2H_6: CH_4 ratio calculated is significantly shifted by approximately +0.06. The average raw C_2H_6: CH_4 ratio for the 15 natural gas events is 0.132 ± 0.007 ppm C_2H_6 /ppm CH_4, while the biogenic events C_2H_6: CH_4 ratio calculated is improbable (-0.02 ± 0.01 ppm C_2H_6 /ppm CH_4).

4.5 Combined method for CH_4 source apportionment

To distinguish which pipeline the emissions originate from, we can compare both the $\delta^{13}CH_4$ signature and the C_2H_6: CH_4 ratio source apportionment methods. The two pipelines were characterised from the whole-air samples taken on July 4th 2014; although the gas within the pipelines is subject to change as incoming gas varies we assume here this did not occur throughout the short duration of the campaign (24th June to the 4th July 2014). The data collected from the aforementioned 16 events is compiled within Fig. 12 which illustrates the distribution of $\delta^{13}CH_4$ signature vs C_2H_6: CH_4 ratios. The results from the flask measurements, i.e. characteristics of Pipeline 1 and 2, are plotted as dashed purple and red lines respectively. Both methods clearly identify the biogenic source, seen as an outlier in the bottom left corner of the plot. Furthermore, both methods are able to distinguish between the two pipelines. The isotopic signatures of the natural gas events (on average 40.2 ‰ ± 0.5‰) are clustered near the isotopic signature of Pipeline 1, which has a $\delta^{13}CH_4$ signature of 40.7 ‰ ± 0.2‰, thus suggesting the majority of the measured methane is an emission from this pipeline. When considering the C_2H_6:CH_4 ratio a similar conclusion may be drawn as the mean C_2H_6:CH_4 ratio is 0.069 ± 0.002 ppm C_2H_6 /ppm CH_4, much alike to that of Pipeline 1 at 0.074 ± 0.003. A future study will address the shift in measured events to left of Pipeline 1 in Fig. 12 by using additional VOC data from the GC-FID to aid source identification. The *uncorrected* 16 events are also plotted in Fig. 12 as circular markers. These are found in the top right hand corner of Fig. 12 and do not correspond well with either of the Pipelines, thus re-confirming the importance of the corrections.

Atmos. Meas. Tech. Discuss., doi:10.5194/amt-2016-261, 2016
Manuscript under review for journal Atmos. Meas. Tech.
Published: 19 December 2016

Atmospheric Measurement Techniques Discussions

496

497 **5. Concluding Remarks**

498 This study focuses on measurements of C_2H_6 contaminated methane sources by a CRDS (Picarro G2201-i), with
499 emphasis on correcting $\delta^{13}CH_4$ and C_2H_6 for cross-interferences before calibration. Our extensive laboratory tests
500 suggest that CRDS instruments of this model are all subject to the similar interferences (as expected as they scan
501 the same spectral lines) and that they can have a significant impact on reported concentrations and isotopic signatures
502 if not accounted for properly, when measuring industrial natural gas sources. We find that the correction coefficients
503 for C_2H_6 and $\delta^{13}CH_4$ do not vary significantly between instruments. For now, we suggest using constant instrument
504 specific correction factors if possible or the ones found in this study (summarised in Fig. 13). As our study period
505 only encompasses one year it is clear that the stability of the correction over the full life-time needs to monitored
506 further. To fully exploit the reported C_2H_6 data, we suggest calibrating the instrument and frequent measurements
507 of a working gas (or set of working gases) to monitor and correct for the instrumental baseline drift.

508 The results of our field campaign demonstrate the extent of the interferences of C_2H_6 on $\delta^{13}CH_4$ for a real world
509 application and also support the validity or our C_2H_6 correction and calibration through the comparison with an
510 independently calibrated GC-FID. In our case, when measuring wet gas emissions we detected an average shift in
511 isotopic signature of 2.5‰ due to C_2H_6 interference, however the extent of this bias will vary according to the
512 contribution of C_2H_6 therefore affecting each ffCH_4 source to a different degree which can cause problems for source
513 determination. The results reported here are important for all future work of CRDS in fossil fuel regions (where
514 sources consist of a C_2H_6:CH_4 ratio between 0-1 ppm C_2H_6/ppm CH_4) to be aware of such interferences and correct
515 for them accordingly. Our CRDS instrument is sufficient for measurements of strongly variable C_2H_6 sources, where
516 if using calibrated one minute C_2H_6 data, concentration variations above 150 ppb are required to achieve a signal to
517 noise ratio of 5. Thus for industrial natural gas sites it offers a new opportunity of using continuous C_2H_6:CH_4
518 observations as a means of source determination independent to $\delta^{13}CH_4$ methods. The recently released G2210-i
519 analyser is dedicated to C_2H_6:CH_4 ratio measurements and as such achieves a higher precision making it suitable
520 for a wider variety of ethane sources.

521 Finally, we successfully combined both the $\delta^{13}CH_4$ and C_2H_6:CH_4 ratio source apportionment methods. At the
522 natural gas compressor site both methods clearly distinguish biogenic sources from that of natural gas based sources.
523 Combining those two independent methods also increases our confidence by giving use a better finger print of the
524 source and spurious C_2H_6 or $\delta^{13}CH_4$ can be more easily identified. Lastly, if we are able to characterise both $\delta^{13}CH_4$
525 and C_2H_6:CH_4 for our source, this gives us insight into the formation and source region of the gas [Schoell, 1983].

526 **Acknowledgements:**

527 The authors would like to thank the NPL team for organising the field campaign, in particular the support from Rod
528 Robinson, Fabrizio Innocenti and Andrew Finlayson. We thank our LSCE colleagues: Camille Yver Kwok and
529 Sebastien Ars for assistance during the field campaign, as well as Bernard Bonsang and Dominique Basinee for

Atmos. Meas. Tech. Discuss., doi:10.5194/amt-2016-261, 2016
Manuscript under review for journal Atmos. Meas. Tech.
Published: 19 December 2016

their technical help and contributions on the GC instruments both in and off the field. We also thank Rebecca Fisher (RHUL) and Dave Lowry for their contributions, especially for measurements of $\delta^{13}CH_4$ for our calibration cylinders under the InGOS' TransNational Access program (TNA-id-666) (http://www.ingos-infrastructure.eu/project-info/workpackages/tna-transnational-access/).. This work was supported by the Climate KIC through the FuME project (http://www.climate-kic.org/projects/fume/) and the funding of the PhD studies of S.A. through education pillar of climate KIC.

Atmos. Meas. Tech. Discuss., doi:10.5194/amt-2016-261, 2016
Manuscript under review for journal Atmos. Meas. Tech.
Published: 19 December 2016

Atmospheric Measurement Techniques Discussions

References:

Allen, D. T. Methane emissions from natural gas production and use: reconciling bottom-up and top-down measurements. Current Opinion in Chemical Engineering, 5, 78-83. (2014).

Bonsang B., and Kanakidou,M. Nonmethane hydrocarbon measurements during the FIELDVOC 1994 experiment, Chemosphere, Global Change Science, 3, 259-273. (2001).

Derwent, R.H., Dernie, J., Dollard, G., Dumitrean, P., Mitchell, R., Murrells, T., Telling, S., Field, R. Twenty years of continuous high time resolution volatile organic compound monitoring in the United Kingdom from 1993 to 2012. Atmospheric Environment 99 (2014) 239-247. (2014).

Fisher, R., Lowry, D., Wilkin, O., Sriskantharajah, S. and Nisbet, G. High- precision, automated stable isotope analysis of atmospheric methane and carbon dioxide using continuous-flow isotope-ratio mass spectrometery. Rapid communications in mass spectrometry, 20(2), 200-208. (2006)

Gilman, J. B., Lerner, B. M., Kuster, W. C., & De Gouw, J. A. Source signature of volatile organic compounds from oil and natural gas operations in northeastern Colorado. Environmental science & technology, 47(3), 1297-1305. (2013).

Gros, V. , Gaimoz,C., Herrmann,F., Custer,T., Williams,J., Bonsang,B., Sauvage,S., Locoge,N., d'Argouges,O., Sarda-Estève,R., and Sciare,J. Volatile Organic Compounds Sources in Paris in spring 2007. Part I: qualitative analysis, Environmental Chemistry, 8, 74-90. (2011).

Hiller, R. V., Bretscher, D., DelSontro, T., Diem, T., Eugster, W., Henneberger, , R. Henneberger, S. Hobi, E. Hodson, D. Imer, M. Kreuzer, T. Künzle, L. Merbold, P. A. Niklaus, B. Rihm, A. Schellenberger[1], M. H. Schroth, C. J. Schubert, H. Siegrist, J. Stieger, N. Buchmann, and D. Brunner. Anthropogenic and natural methane fluxes in Switzerland synthesized within a spatially explicit inventory. Biogeosciences, 11(7), 1941-1959. (2014).

Höglund-Isaksson, L. Global anthropogenic methane emissions 2005–2030: technical mitigation potentials and costs. Atmospheric Chemistry and Physics, 12(19), 9079-9096. (2012).

Jackson, R. B., Down, A., Phillips, N. G., Ackley, R. C., Cook, C. W., Plata, D. L., & Zhao, K. Natural gas pipeline leaks across Washington, DC. Environmental science & technology, 48(3), 2051-2058. (2014)

Miller, J.B., and Tans, P.P. "Calculating isotopic fractionation from atmospheric measurements at various scales." Tellus B 55.2 (2003): 207-214. (2003).

572
573 Kirschke, S., Bousquet, P., Ciais, P., Saunois, M., Canadell, J. G., Dlugokencky, E. et al. Three decades of global
574 methane sources and sinks. Nature Geoscience, 6(10), 813-823. (2013).
575
576 Lamb, B. K., McManus, J. B., Shorter, J. H., Kolb, C. E., Mosher, B., Harriss, R. C., Allwine,E., Blaha, D.,
577 Howard,T., Guenther,A., Lott, R. A., Siverson,R., Westburg, H., Zimmerman,P. Development of atmospheric
578 tracer methods to measure methane emissions from natural gas facilities and urban areas. Environmental science
579 & technology, 29(6), 1468-1479. (1995).

580 Laurent, O et al. "Icos ATC Metrology Lab: Metrological performance assessment of GHG analyzers."
581 Atmospheric Measurement Techniques 8.10 (2015): 4075-4082. Poster session presented at: 18th WMO/IAWA
582 Meeting on Carbon Dioxide, Other Greenhouse Gases, and Related Measurement Techniques (GGMT). Sep 13-
583 17. 2015; California, CA.

584 Lowry, D., Holmes, C. W., Rata, N. D., O'Brien, P., & Nisbet, E. G. London methane emissions: Use of diurnal
585 changes in concentration and δ13C to identify urban sources and verify inventories. Journal of Geophysical
586 Research: Atmospheres, 106(D7), 7427-7448. (2001).

587 Malowany, K., Stix, J., Van Pelt, A., & Lucic, G. H 2 S interference on CO 2 isotopic measurements using a
588 Picarro G1101-i cavity ring-down spectrometer. Atmospheric Measurement Techniques, 8(10), 4075-4082.
589 (2015).

590 Nara, H., Tanimoto, H., Tohjima, Y., Mukai, H., Nojiri, Y., Katsumata, K., & Rella, C. W. Effect of air
591 composition (N 2, O 2, Ar, and H 2 O) on CO 2 and CH 4 measurement by wavelength-scanned cavity ring-down
592 spectroscopy: calibration and measurement strategy. Atmospheric Measurement Techniques, 5(11), 2689-2701.
593 (2012).

594 Phillips, N. G., Ackley, R., Crosson, E. R., Down, A., Hutyra, L. R., Brondfield, M., Karr,J.D., Zhao, K.,
595 Jackson, R. B. Mapping urban pipeline leaks: Methane leaks across Boston. Environmental pollution, 173, 1-4.
596 (2013).

597 Rella, C. W., Hoffnagle, J., He, Y., & Tajima, S. Local-and regional-scale measurements of CH 4, δ 13 CH 4, and
598 C 2 H 6 in the Uintah Basin using a mobile stable isotope analyzer. Atmospheric Measurement Techniques, 8(10),
599 4539-4559. (2015).

600 Roscioli, J. R., Yacovitch, T. I., Floerchinger, C., Mitchell, A. L., Tkacik, D. S., Subramanian, Martinez, D. M.,
601 Vaughn, T. L., Williams, L., Zimmerle, D., Robinson, A. L., Herndon, S. C., & Marchese, A. J. Measurements of
602 methane emissions from natural gas gathering facilities and processing plants: measurement methods.
603 Atmospheric Measurement Techniques, 8(5), 2017-2035. (2015).

604 Schoell, M. Genetic characterization of natural gases. AAPG bulletin, 67(12), 2225-2238. (1983).

605 Smith, M. L., Kort, E. A., Karion, A., Sweeney, C., Herndon, S. C., & Yacovitch, T. I. Airborne ethane
606 observations in the Barnett shale: Quantification of ethane flux and attribution of methane emissions.
607 Environmental science & technology, 49(13), 8158-8166. (2015).

608 Stevens, C. M., & Engelkemeir, A. Stable carbon isotopic composition of methane from some natural and
609 anthropogenic sources. Journal of Geophysical Research: Atmospheres, 93(D1), 725-733. (1988).
610
611 Subramanian, R., Williams, L. L., Vaughn, T. L., Zimmerle, D., Roscioli, J. R., Herndon, S. C., Yacovitch, T.L.,
612 Floerchinger, C., Tkacik, D.S., Mitchell, A.L., Sullivan, M. R., Dallmann, T.R., & Robinson, A.L. Methane
613 emissions from natural gas compressor stations in the transmission and storage sector: Measurements and
614 comparisons with the EPA greenhouse gas reporting program protocol. Environmental science & technology,
615 49(5), 3252-3261. (2015).
616

617 U.S Environmental Protection Agency. "Inventory of U.S Greenhouse Gas Emissions and Sinks: 1990-2014. "
618 EPA 430-R-16-002 (2016): Annex 7. Found online here:
619 https://www3.epa.gov/climatechange/Downloads/ghgemissions/US-GHG-Inventory-2016-Annex-7-
620 Uncertainty.pdf

621 Vogel, F. R., Huang, L., Ernst, D., Giroux, L., Racki, S., & Worthy, D. E. J. Evaluation of a cavity ring-down
622 spectrometer for in situ observations of 13 CO 2. Atmospheric Measurement Techniques, 6(2), 301-308. (2013).

623 Waked, A., Sauvage, S., Borbon, A., Gauduin, J., Pallares, C., Vagnot, M., Leonardis, T., Locoge, N. Multi-year
624 levels and trends of non-methane hydrocarbon concentrations observed in ambient air in France. Atmospheric
625 Environment 141 (2016) 263-275. (2016).

626 Yacovitch, T. I., Herndon, S. C., Roscioli, J. R., Floerchinger, C., McGovern, R. M., Agnese, M., Pétron, G.,
627 Kofler, J., Sweeney, C., Karion, A., Conley, S. A., Kort, E. A., Nähle,L., Fischer, M., Hildebrandt,L., Koeth,J.,
628 McManus, J. B., Nelson, D. D., Zahniser, M. S., & Kolb. C. E. Demonstration of an ethane spectrometer for
629 methane source identification. Environmental science & technology, 48(14), 8028-8034. (2014).

630 Yacovitch, T. I., Herndon, S. C., Pétron, G., Kofler, J., Lyon, D., Zahniser, M. S., & Kolb, C. E. Mobile laboratory
631 observations of methane emissions in the Barnett Shale region. Environmental science & technology, 49(13),
632 7889-7895. (2015).

633 York, D. Least squares fitting of a straight line with correlated errors. Earth and Planetary Science Letters 5,
634 (1969), 320-324. (1968).

Atmos. Meas. Tech. Discuss., doi:10.5194/amt-2016-261, 2016
Manuscript under review for journal Atmos. Meas. Tech.
Published: 19 December 2016

635 Yvon-Lewis, S. A., Hu, L., & Kessler, J. Methane flux to the atmosphere from the Deepwater Horizon oil disaster.
636 Geophysical Research Letters, 38(1). (2011).

Atmos. Meas. Tech. Discuss., doi:10.5194/amt-2016-261, 2016
Manuscript under review for journal Atmos. Meas. Tech.
Published: 19 December 2016

Table 1: Description of the gas mixtures used to determine the cross-sensitivities of the interference of CH_4, H_2O and CO_2 on C_2H_6 and the interference of C_2H_6 on $\delta^{13}CH_4$. The respective ranges spanned during laboratory tests, and the typical range at a natural gas site are noted in the right hand side.

		Method	Dilution Gas	Working Gas	Lab Concentration Range	Typical Range at NG site
H_2O Interference on C_2H_6	<0.16% (Dry)	Magnesium Perchlorate	N/A	Ambient Air	0-0.5% H_2O	0-2% H_2O
	≥0.16% (Wet)	Dilution Series & Humidifier		Zero Air	0.25-2.5% H_2O	
CO_2 Interference on C_2H_6	<0.16% (Dry)	Dilution Series	Zero Air	2000ppm CO_2, 1.7ppm CH_4, < 1ppb C_2H_6 and 50ppb CO in natural air	0-1500ppm CO_2	400-1000 ppm CO_2
	≥0.16% (Wet)	Dilution Series & Humidifier			0-1500ppm CO_2, 0.5-1.5 % H_2O	
CH_4 Interference on C_2H_6	<0.16% (Dry)	Dilution Series & Ascarite	Zero Air	6ppm CH_4, 360ppm CO_2, 310ppb N_2O, < 1ppb C_2H_6 and 50ppb CO in natural air	0-6ppm CH_4	2-20 ppm CH_4
	≥0.16% (Wet)	Dilution Series, Ascarite & Humidifier			0-6ppm CH4, 1%H_2O	
C_2H_6 Interference on $\delta^{13}CH_4$		Dilution Series (CRDS)	Natural Air Matrix (<1ppb C_2H_6)	C_2H_6 standard of 52ppm in Nitrogen	0-1.5 ppm C_2H_6 /ppm CH_4	0-0.3 ppm C_2H_6/ ppm CH_4
C_2H_6 Calibration		Dilution Series (CRDS & GC)	Natural Air Matrix (<1ppb C_2H_6)	C_2H_6 standard of 52ppm in Nitrogen	0-5ppm C_2H_6	0.3-3 ppm C_2H_6

Atmos. Meas. Tech. Discuss., doi:10.5194/amt-2016-261, 2016
Manuscript under review for journal Atmos. Meas. Tech.
Published: 19 December 2016

Atmospheric Measurement Techniques Discussions

Table 2: Summary of C_2H_6 calibration factors calculated for both instruments CFIDS 2072 and 2067.

C_2H_6 Calibration	CFIDS 2072		CFIDS 2067	
	Slope	**Intercept (ppm)**	**Slope**	**Intercept (ppm)**
Feb,15	0.49 ± 0.03	0.00 ± 0.01		
Oct,15	0.51 ± 0.01	-0.06 ± 0.04	0.52 ± 0.01	-0.12 ± 0.01

Table 3: The various response functions calculated for the $\delta^{13}CH_4$ correction due to C_2H_6. *Flask measurement.

$\delta^{13}CH_4$ Correction	CFIDS 2072		CFIDS 2067	
	Slope(‰CH_4/C_2H_6)	**Intercept (‰)**	**Slope(‰CH_4/C_2H_6)**	**Intercept (‰)**
July,15	+24 ± 2	0.5 ± 0.6	-	-
Nov,15	+23 ± 1	0.2 ± 0.6	+23 ± 1	-2.3 ± 0.7
Nov,15 *	+24 ± 1	0.6 ± 0.6	+24 ± 2	-2.5 ± 0.8

Atmos. Meas. Tech. Discuss., doi:10.5194/amt-2016-261, 2016
Manuscript under review for journal Atmos. Meas. Tech.
Published: 19 December 2016

Atmospheric Measurement Techniques Discussions

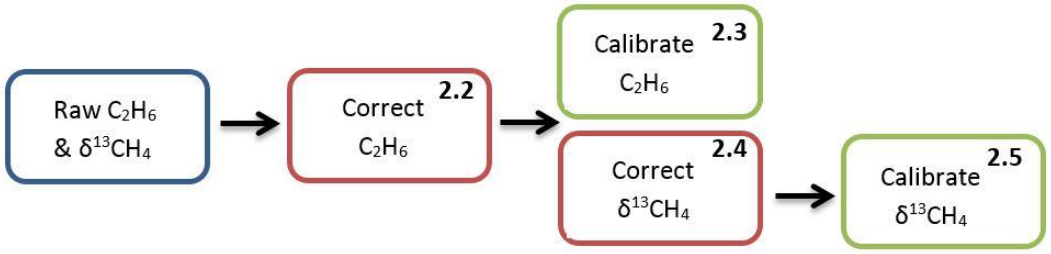

Figure 1: Flow chart illustrating the steps involved to calibrate C_2H_6, and $\delta^{13}CH_4$. The number in the top right hand corner corresponds to the subsection in which the methods of each step are explained in detail.

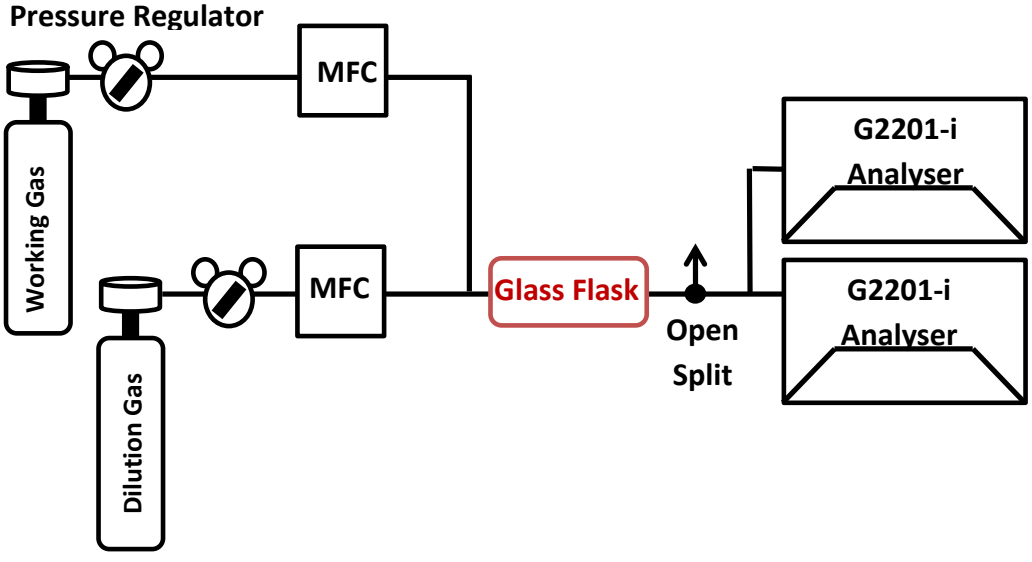

Figure 2: General Set-up. The dilution and working gas are connected via two MFCs to two CRDS instruments in parallel. In red is the placement of an optional glass flask used for the C_2H_6 calibration only. The flow is greater than that of the instruments inlets, therefore an open split is included to vent additional gas and retain ambient pressure at the inlets.

Atmos. Meas. Tech. Discuss., doi:10.5194/amt-2016-261, 2016
Manuscript under review for journal Atmos. Meas. Tech.
Published: 19 December 2016

Atmospheric Measurement Techniques Discussions

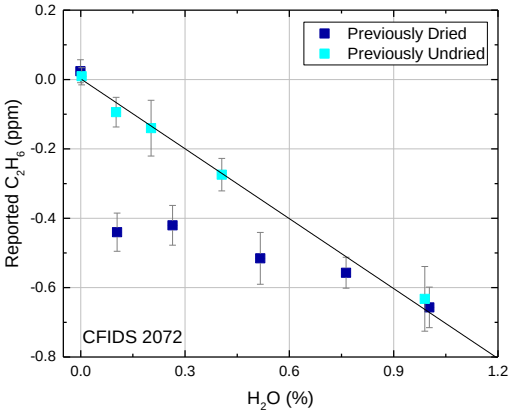

Figure 3: An example of the results from a H_2O interference experiment spanning the range 0-1% H_2O. The reported C_2H_6 is altered due to the addition of water vapour when measuring zero air (<1ppb C_2H_6). Dark and light blue markers signify the response when dried and undried ambient air have been measured overnight by the instrument prior to the experiment respectively. Error bars signify the standard deviation of each measurement.

Atmos. Meas. Tech. Discuss., doi:10.5194/amt-2016-261, 2016
Manuscript under review for journal Atmos. Meas. Tech.
Published: 19 December 2016

Atmospheric Measurement Techniques Discussions

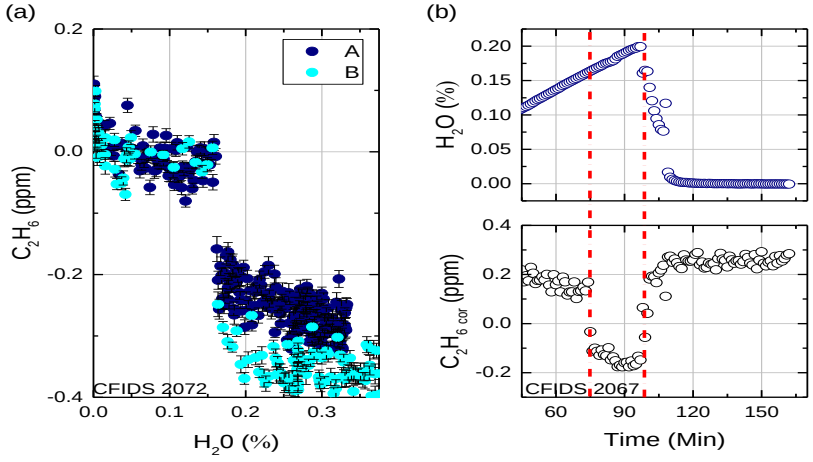

Figure 4(a): The discontinuity seen for instrument CFIDS 2072 for two repetitions denoted by different colours. After the discontinuity at 0.16% the subsequent slope clearly differs between the two repetitions. Both instruments display a discontinuity at 0.16% H_2O. Each point represents a one minute average, the error bars represent the standard deviation of the raw data.

Figure 4(b): Time series of the discontinuity for instrument CFIDS 2067, the H_2O content is increased and decreased crossing the 0.16% H_2O threshold twice. The point at which 0.16% H_2O humidity is reached is marked by red dashed lines. The discontinuity is present when moving from dry to wet air, and inversely from wet to dry air.

Atmos. Meas. Tech. Discuss., doi:10.5194/amt-2016-261, 2016
Manuscript under review for journal Atmos. Meas. Tech.
Published: 19 December 2016

Atmospheric Measurement Techniques Discussions

46

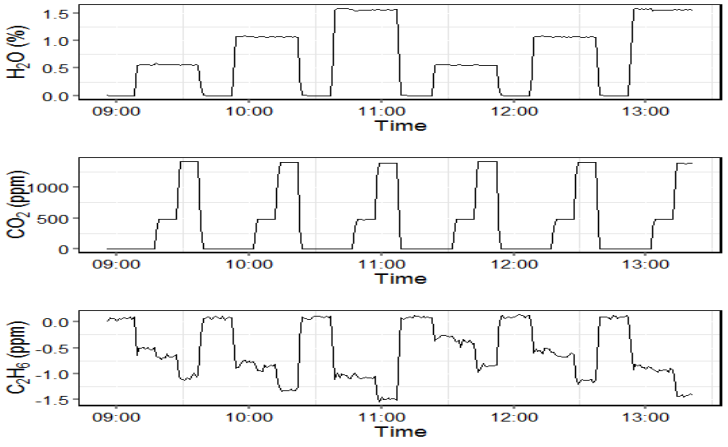

54

55

56 Figure 5: Time series of CO_2 interference experiment at varying H_2O concentrations. As H_2O and CO_2 are altered,
57 the reported C_2H_6 is expected to be constant given there is no C_2H_6 input. However due to interference the
58 corresponding shifts of reported C_2H_6 are evident

59

60

61

Atmos. Meas. Tech. Discuss., doi:10.5194/amt-2016-261, 2016
Manuscript under review for journal Atmos. Meas. Tech.
Published: 19 December 2016

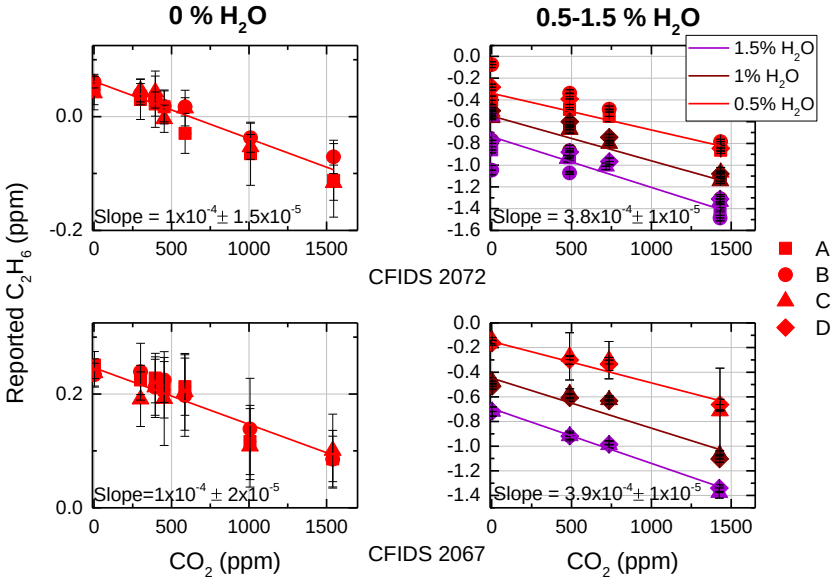

62

63 Figure 6: Relationship between reported C_2H_6 and concentration changes of CO_2 for instrument CFIDS 2072 and
64 2067 at varying values of H_2O. For each plot the bottom axis indicates the increase in concentration of the targeted
65 gas (CO_2). Plots on the left are at 0% H_2O, on the right are experiments at varying humidities, distinguishable by
66 colour. The legend denotes repetitions of the experiment. The error bars in each plot denote the standard deviation
67 of each measurement. The R^2 value for the experiments at 0% H_2O is 0.9 and 0.8 for all other H_2O experiments for
68 both instruments.

Atmos. Meas. Tech. Discuss., doi:10.5194/amt-2016-261, 2016
Manuscript under review for journal Atmos. Meas. Tech.
Published: 19 December 2016

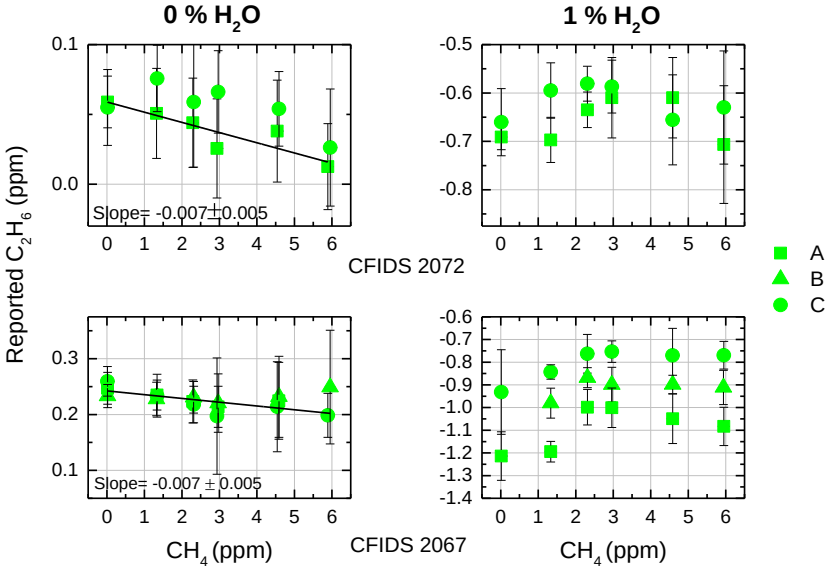

Figure 7. Relationship between reported C_2H_6 and concentration changes of CH_4 for both instruments. For each plot, the bottom axis indicates the increase in concentration of the targeted gas. The vertical bars in each plot denote the standard deviation of each point. The legend denotes repetitions of the experiment. Plots on the left are at 0% H_2O. The R^2 value is 0.4 and 0.6 for instruments CFIDS 2072 and 2067 respectively. Plots on the right show the response at 1% H_2O. These two plots have a R^2 value of 0.2.

Atmos. Meas. Tech. Discuss., doi:10.5194/amt-2016-261, 2016
Manuscript under review for journal Atmos. Meas. Tech.
Published: 19 December 2016

Atmospheric Measurement Techniques Discussions

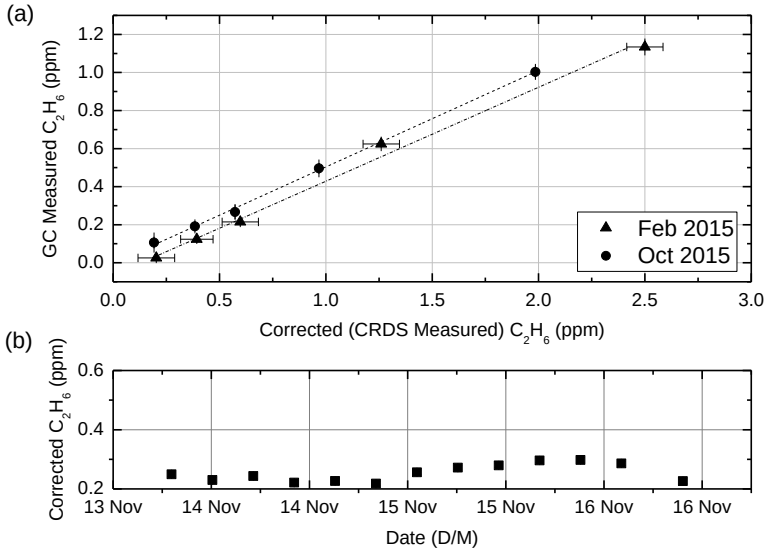

Figure 8(a): Ethane calibration calculated from measurements of flask samples by both the GC and CRDS. The x-axis is the corrected C_2H_6 ($C_2H_{6\,COR}$) using the corrections described previously. The y-axis is the C_2H_6 as measured by a manual GC. The error bars indicate the standard deviation of each flask measurement, for certain flasks error bars are smaller than their respective markers.

Figure 8(b): 30 minute target measurements over a period of 4 days, from 13th November 2015, to 16th November 2015. The standard error of each target is smaller than the plotted marker. The baseline C_2H_6 is seen to drift with time.

Atmos. Meas. Tech. Discuss., doi:10.5194/amt-2016-261, 2016
Manuscript under review for journal Atmos. Meas. Tech.
Published: 19 December 2016

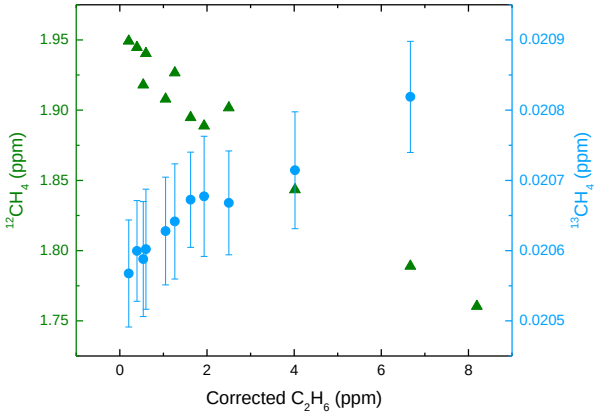

Figure 9: During a dilution sequence, the CH_4 concentration is manually decreased as the contribution from C_2H_6 is increased. Thus both $^{12}CH_4$ and $^{13}CH_4$ undergo a similar decrease as the gas is diluted. However what is observed is an increase in the reported value of $^{13}CH_4$, suggesting C_2H_6 interference. The nominal CH_4 concentration of the ambient gas is 1948.7ppb ± 0.32 ppb. The $^{12}CH_4$ axis is plotted to the left in light green, whereas the $^{13}CH_4$ axis is plotted to the right in dark green at a different scale. Error bars represent the standard deviation, the $^{12}CH_4$ markers are larger than their associated error bars.

Atmos. Meas. Tech. Discuss., doi:10.5194/amt-2016-261, 2016
Manuscript under review for journal Atmos. Meas. Tech.
Published: 19 December 2016

Atmospheric Measurement Techniques Discussions

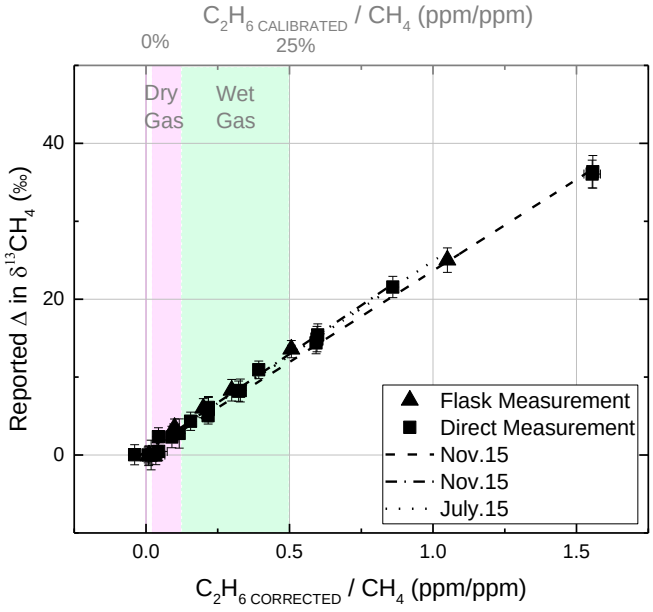

97

98 Figure 10: The effect of C_2H_6 on reported $\delta^{13}CH_4$. The slopes of reported $\delta^{13}CH_4$ vs the $C_2H_{6\ CORRECTED}$:CH_4 ratio
99 are shown for three tests taken throughout the course of one year. Triangular markers imply whole air sample
100 measurements, while square markers are derived from direct measurements. Error bars indicate the standard
101 deviation. In the presence of C_2H_6 the instrument reports heavier values of $\delta^{13}CH_4$. The typical range of
102 (calibrated) C_2H_6 : CH_4 of dry and wet gas is highlighted in pink and green respectively corresponding to the top
103 axis.

104

Atmos. Meas. Tech. Discuss., doi:10.5194/amt-2016-261, 2016
Manuscript under review for journal Atmos. Meas. Tech.
Published: 19 December 2016

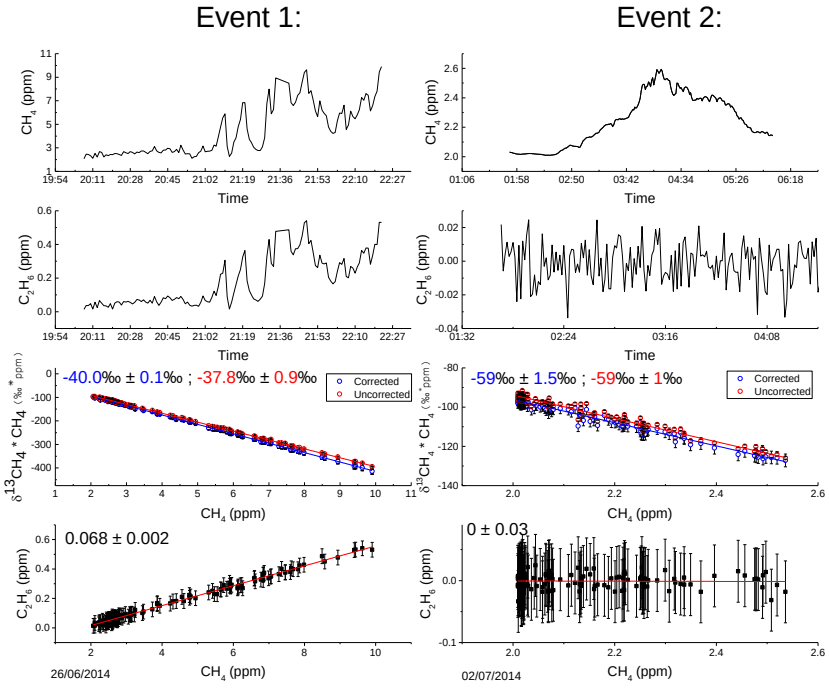

Figure 11: Ethane and Methane content of two selected peaks. Methane and Ethane 1 minute averaged time series is shown in the top two panels. Miller-Tans plots of the corresponding peaks are shown in the third panel, blue for the corrected $\delta^{13}CH_4$ due to C_2H_6, and red representing uncorrected $\delta^{13}CH_4$. Event 1 includes elevated C_2H_6 emissions and thus displays a difference between the slope before and after C_2H_6 correction, corresponding to a shift in isotopic signature. Event 2, with no C_2H_6 shows no alteration in slope. The slopes of C_2H_6 vs CH_4 are shown in the bottom panel, signifying the C_2H_6: CH_4 ratio of the emission. Error of both the isotopic and C_2H_6: CH_4 signatures are calculated from the standard error of the slope.

Atmos. Meas. Tech. Discuss., doi:10.5194/amt-2016-261, 2016
Manuscript under review for journal Atmos. Meas. Tech.
Published: 19 December 2016

Atmospheric Measurement Techniques Discussions

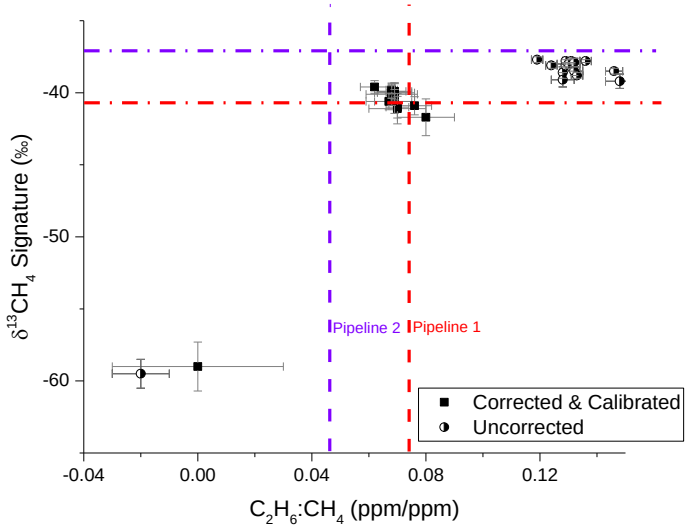

Figure 12: Distribution of 16 events according to their C_2H_6: CH_4 ratios and isotopic signature. The red and purple dashed lines signify the characterisation of Pipeline 1 and 2 respectively as measured by the CRDS instrument from flask samples taken on the 4.07.14. For corrected and calibrated data (square markers), both the isotopic signature and C_2H_6: CH_4 ratios identify the biogenic source (bottom-left point) and suggest the natural gas emissions emanate from Pipeline 1. Circular markers represent the uncorrected data which does not agree with the flask sample measurements of Pipelines 1 or 2. The error bars indicate the standard error of the slope calculated from Miller-Tans and C_2H_6 vs CH_4 plots for $\delta^{13}CH_4$ signature and C_2H_6: CH_4 ratio respectively.

Atmos. Meas. Tech. Discuss., doi:10.5194/amt-2016-261, 2016
Manuscript under review for journal Atmos. Meas. Tech.
Published: 19 December 2016

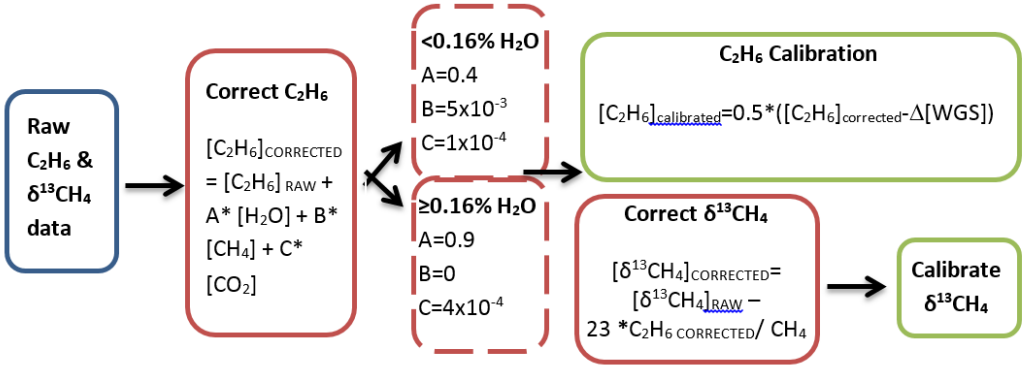

131

132

133 Figure 13: Flow chart illustrating the steps and the corresponding equations to calibrate C_2H_6 and $\delta^{13}CH_4$ as
134 determined from this study. The coefficients are the mean of both CRDS instruments tested.